

https://dspace.org/

Investigation of mechanical properties and the effect of volume fraction of polycrylamide hydrogel with molecular dynamics simulation

NK Dehkordi; S Shojaei; A Asefnejad; Kamran Hassani; Soheil Z Benisi

https://hdl.handle.net/10539/43748
WOS

Downloaded from a DSpace repository. https://dspace.org/

Results in Physics 57 (2024) 107440



Contents lists available at ScienceDirect

Results in Physics

journal homepage: www.elsevier.com/locate/rinp

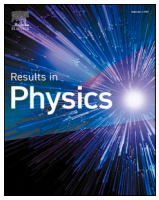



Investigation of mechanical properties and the effect of volume fraction of polyacrylamide hydrogel with molecular dynamics simulation

Narges Karimzadeh Dehkordi [a], Shahrokh Shojaei [b,c,*], Azadeh Asefnejad [a], Kamran Hassani [a], Soheila Zamanlui Benisi [b,c]

[a] Department of Biomedical Engineering, Science and Research Branch, Islamic Azad University, Tehran, Iran
[b] Department of Biomedical Engineering, Islamic Azad University, Central Tehran Branch, Tehran, Iran
[c] Stem Cell Research Center, Tissue Engineering and Regenerative Medicine Institute, Central Tehran Branch, Islamic Azad University, Tehran 13185/768, Iran

ARTICLE INFO

Keywords:
Hydrogel
Molecular dynamics simulation
Mechanical properties
Young's modulus
Polyacrylamide

ABSTRACT

Hydrogels use three-dimensional polymer networks with transverse connections as their technology to absorb water or biofluids. Water, as a fundamental component, significantly affects the functionality of biomedical polymers, including hydrogels. The molecular organization of water within hydrogels and its state (limited, medium, or free) were significant factors in biocompatibility and compatibility. If hydrophilic monomers are directly used to produce the product, the manufactured product will have poor mechanical properties. Consequently, it is critical to conduct research on the mechanical properties of hydrogels, as well as methods for increasing them. This study examined the interactions between polyacrylamide hydrogel and water molecules by studying the effect of different volume fractions (5–15 %) of polyacrylamide hydrogel on the mechanical properties (Young's modulus and ultimate strength) using molecular dynamics simulation. The results show that the potential and total energy in the sample converged to −43 and 12488 kcal/mol. The ultimate strength of sample was 0.0333 MPa. The Young's modulus calculated for polyacrylamide was 0.0009 MPa. By increasing the atomic ratio of structure in the range of 5 % to 15 %, the ultimate strength value increased from 0.0333 MPa to 0.0425 MPa. The value of Young's modulus reached its maximum, from 0.0009 MPa to 0.0014 MPa.

Introduction

Three-dimensional polymer networks called hydrogels have a very high capacity to bind water or other biofluids. These substances are capable of adsorbing water up to 1000 times greater than the mass of polymer without dissolving. The soft surface, structure, and physicochemical properties of hydrogels are comparable to those of biological components [1–3]. Hydrogels are created via physical and chemical processes, and the hydrophilic functional groups in polymer chains, such as COOH, $–NH_2$, –OH, $–CONH_2$, and $–SO_3H$ groups, are what give hydrogels their ability to adsorb water. Despite the fact that cross-connections across network chains prevent them from dissolution [4]. Many natural and synthetic materials are classified as hydrogels. Synthetic hydrogels have gradually replaced natural hydrogels in the last two decades in terms of their high water absorption capacity, and higher structural strength [5]. Hydrogels have various applications, including biomedical, bioengineering, biosensors, tissue engineering, and cell separation [4,6]. The mechanical properties (MP) of hydrogels have a critical role in regulating the phenotype and genotype of cells, as well as how they interact with the extracellular matrix. While significant progress was made in adjusting the bio MP of hydrogels, challenges still lie in synthesizing them with complex mechanical profiles, and vascularization and modeling of natural tissues' complex structures remain limited, impeding the development of complex organs [7,8].Therefore, advanced methods and techniques are of particular importance to measure different types of various bio MP of hydrogels, and new methods to increase their biomechanics. Jefari et al. [9] investigated the MP of Polyacrylamide (PAA)/gelatin hydrogel. The results show that the swelling ratio of the hydrogels was 947 %, while the modulus varied between 5 and 35 kPa. Olaret et al. [10] studied the MP of PAA-acrylamide-carbon nanotubes/Ag hydrogel. The results show that adding PAA to the hydrogel improved the MP. Most of the experimental methods used to measure the MP of hydrogels were time-consuming and

Abbreviations: PAA, polyacrylamide; MP, mechanical properties; YM, young's modulus; US, ultimate strength; MD, molecular dynamics; LJ, Lennard-Jones; LAMMPS, large-scale atomic/molecular massively parallel simulation.

* Corresponding author.
E-mail address: s.shojaei@aut.ac.ir (S. Shojaei).

https://doi.org/10.1016/j.rinp.2024.107440
Received 19 May 2023; Received in revised form 6 January 2024; Accepted 1 February 2024
Available online 6 February 2024
2211-3797/© 2024 The Author(s). Published by Elsevier B.V. This is an open access article under the CC BY license (http://creativecommons.org/licenses/by/4.0/).

Nomenclature

r_{ij}	The distance between particles (m)
u_i	The potential of a particle (eV)
ε_{ij}	Depth of the potential well (Kcal/mol)
σ_{ij}	Finite distance in which the potential is zero(Å)
r	The distance of the particles from each other
U_{ij}	The electric potential (eV)
V	The total volume of particles (Å^3)
m_i	The mass of the particle(g)
a_i	The acceleration of the particle (m·s^{-2})

expensive. They did not have the possibility to predict the properties under other conditions. Consequently, it was possible to examine the structure and behavior of materials using computer simulation, which was one of the most effective methods.

Frequently, these methods analyze the conduct of the system's components, such as molecules and tiny particles, and thereafter deduce the necessary macroscopic and microscopic quantities from their findings [11]. To determine whether a compound was stable under present conditions, experimental methods were used. Molecular simulation methods, such as Molecular Dynamics (MD) simulation, can be used for unstable compounds, as well as compounds that are yet to be identified [12]. An et al. [13] studied the simulation and estimation of the mechanical and thermal properties of PAA. Based on all-atom MD simulations, this study determined that the hydrogel's elasticity was strongly dependent on the polymer content fraction. Xu et al. [14] investigated the MP of TM-SiO_2/PAM/PAA nanocomposite. According to the findings, TM-SiO_2/PAM/PAA nanocomposite's compressive stress was 7.01 MPa. Their findings showed that the hydrogel's strength was increased by adding hydroxyapatite (HAP). Using MD simulation, Dehkordi et al. [15] studied the swelling and heating behavior of three cross-linked hydrogels (PAA, polyvinyl alcohol, and polyethylene glycol). The findings show that PAA had superior thermal and atomic behavior. Using MD simulation, Liu et al. [16] investigated the MP of a physicochemical hybrid hydrogel. According to the findings, a chain-length ratio of 7:1:7 was ideal for obtaining the best MP of this hybrid hydrogel. Using MD modeling, Shahshahani et al. [17] examined the effect of volume fraction and initial temperature on the MP of methacrylic acid porous hydrogels. The results indicate that the Young's modulus (YM) and ultimate strength (US) increase from 247 MPa and 131 to 274 MPa and 146 MPa, respectively, when the volume fraction increased from 5 to 15 %. Using MD simulation, Koochaki et al. examined the MP of polyethylene glycol hydrogel/ cellulose nanofibrils. According to the results, when 3 % cellulose nanofibrils were included, the US and YM of the proposed nanocomposite increased to 0.26 MPa and 0.39 MPa, respectively.

Water, as a fundamental component, significantly affects the functionality of biomedical polymers, including hydrogels. The molecular organization of water within hydrogels and its state (limited, medium, or free) were significant factors in biocompatibility and compatibility [18]. If hydrophilic monomers were directly used to produce the product, the manufactured product would have poor MP [19]. Consequently, it is critical to conduct research on the MP of hydrogel, as well as methods for increasing it. Previous studies [17] identified the volume fraction of hydrogel as a factor that affects its MP. This research examined the interactions between PAA hydrogel and water molecules by studying the effect of different volume fractions (5–15 %) of PAA hydrogel on the MP (YM and US) using MD simulation.

Present simulation details

This study considered a box with the simulation dimensions of 100 × 100 × 200 Å^3. 200 Å length in Z direction was implemented to the atomic structure can be fluctuated arbitrary and this parameter decreased to 100 Å after geometry optimization. Water was simulated by the (SPC) potential model and the hydrogel structures of PAA by the Avogadro software. To implement these processes, the initial and final temperature and pressure settings must be specified. In order to achieve this objective, the Noz-Hoover thermostat was used to set Temp = 300 K and P = 1 bar of the structure. The simulation was then conducted using the LAMMPS software. Fig. 1 displays a schematic of the simulated structure.

The equilibrium was achieved using a constant pressure–temperature ensemble (NPT) [23]. The equilibrium of structures was assessed at 2 ns. The equilibrium process time of the structures was incorporated into the simulation time, which was 7 ns at a time increment of 1 fs. Once the atomic stability of the simulated structures was verified, the percentage of hydrogel swelling was computed. The percentage of hydrogel swelling in distilled water was computed using Eq. (1):

$$S\% = \frac{m - m_0}{m_0} \times 100 \tag{1}$$

m_0 represents the mass of the swollen gel at time zero, while m represents the mass of the expanded gel at time t. A period of time was spent monitoring the water absorption of initially dried hydrogels until they reached their maximal swelling.

Results and discussion

Equilibrium atomic samples

To establish the thermodynamic equilibrium of the simulated atomic structures, the initial stage included investigating the physical properties of the simulated systems, such as potential energy and total energy. Fig. 2 displays the change in potential energy of the PAA atomic sample during a duration of 10 ns. The stability of atomic sample was determined using the potential energy value. Stable atomic structures, such as solids, have a negative value for this parameter. In this section, we illustrate how the structure's potential energy converged by increasing simulation time. The potential energy of the PAA reached a value of −43 Kcal/mol after a convergence period of 10 ns. The atomic sample showes a negative potential energy in terms of the attraction force inside its structure.

Fig. 3 illustrates the total changes in the energy of PAA during a

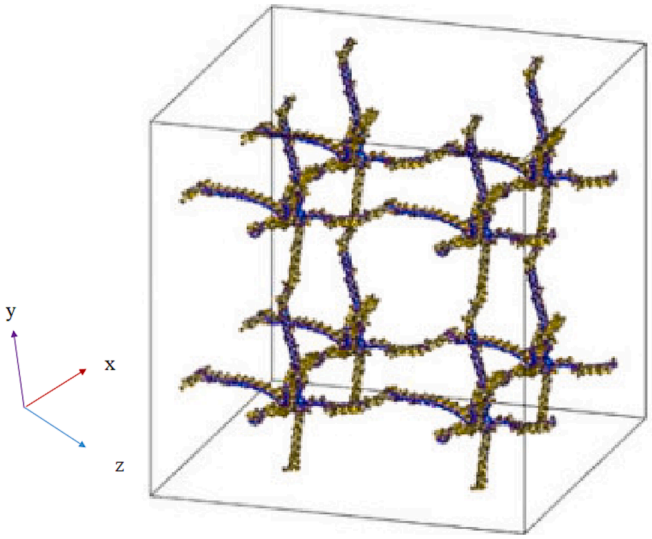

Fig. 1. A schematic of the simulated structure.

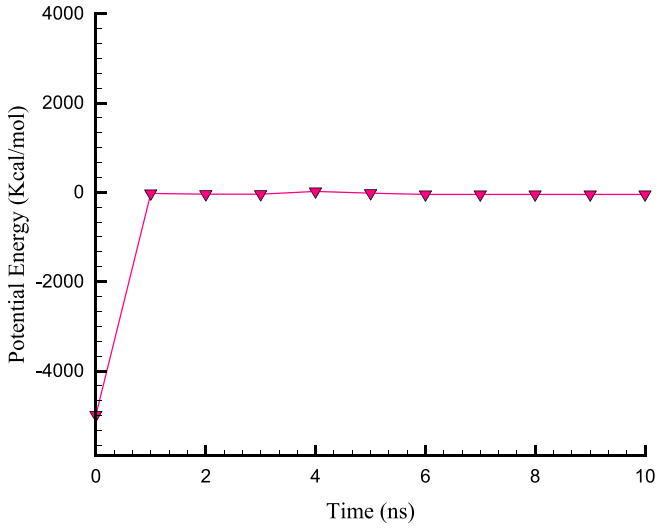

Fig. 2. Potential energy changes of PAA atomic sample after 10 ns.

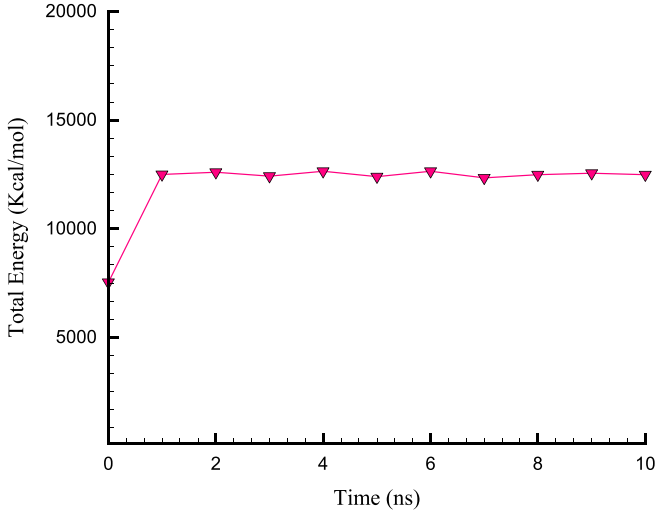

Fig. 3. Total energy changes of PAA atomic sample after 10 ns.

period of 10 ns. The sum of the kinetic and potential energies of an atomic sample signified its total energy. The cumulative energy of the atomic sample reached 12,488 Kcal/mol after a duration of 10 ns. Convergence in the total energy of the PAA structure showed that the kinetic energy was larger than the potential energy of the samples, owing to the high mobility of water molecules, and did not suggest disequilibrium in the final sample. On the other hand, a certain value that converged for this physical quantity showed the attraction force of structures. Based on the results obtained in the equilibrium stage of the structures, the potentials used in this study were suitable to investigate the structural evolution of PAA.

Mechanical behavior of PAA

Fig. 4 depicts the stress–strain diagram of PAA at Temp = 300 K and P = 1 bar. The sample was exposed to external stress with a strain rate of 0.01 s^{-1}. The results demonstrate the enhanced MP of PAA, as shown in the sample's ultimate strain of 23.1 and stress of 0.0333 MPa. This improvement in the MP of PAA hydrogel increased its use in different medical applications, including ophthalmology. However, from a physical viewpoint, the explanation for the improved behavior of PAA hydrogel was the attractive contact among the atoms of this material, which worked as an atomic skeleton and made the final PAA material stronger.

YM value of the structure was determined by calculating the slope of the stress–strain diagram in the linear area. Fig. 5 displays the YM of the PAA at 300 K and 1 bar. For PAA, the calculated value of YM was 0.0009 MPa.

Table 1 shows the US YM of PAA at 300 K and 1 bar after 10 ns.

Effect of hydrogel volume fraction

The changes in the volume fraction directly affected the MP of different structures. To examine this issue, the atomic ratios used in the current study were 5 %, 10 %, and 15 %. Nevertheless, since PAA was an ideal hydrogel, we expect that the results were applicable to other hydrogels as well. The US of simulated PAA based on the atomic ratio is illustrated in Fig. 6 at 300 K and 1 bar. By raising the structure's atomic ratio from 5 % to 15 %, the US value rose from 0.0333 MPa to 0.0425 MPa. The mechanical resistance of sample was improved by increasing the atomic ratio of hydrogel. To ensure the general pattern which shown in Figs. 6 and 7, the atomic ratio changed to smaller (1 %) and larger (30 %) values. MD outputs predicted 0.0284 MPa and 0.0008 MPa for US and YM parameters when atomic ratio set to 1 %. Furthermore, these parameters converged to 0.0477 MPa and 0.0018 MPa (respectively) in atomic ratio with 30 % value. The increased mechanical strength of samples was attributed to the higher concentration of hydrogel in the aqueous environment, which was a consequence of the increased interatomic attraction force resulting from the reduced interatomic distance in the samples. Physically, the potential energy in the samples was inversely related to the interatomic distance. Therefore, when the structures became denser, the distance among the atoms decreased, leading to an increase in the interatomic attraction force. Consequently, the sample became more physically stable. The results align with the results reported by Shahshahani et al. [17]. The results indicate that by increasing the volume percentage from 5 to 15 %, YM and US saw an increase from 247 MPa and 131 MPa to 274 MPa and 146 MPa, respectively.

YM diagram of a simulated PAA hydrogel sample at 300 K and 1 bar is depicted in Fig. 7. The greatest value of YM was observed to be 0.0014 MPa from 0.0009 MPa. The specified hydrogel's number of atoms and absorption power grew as the volume percentage of hydrogel increased. This resulted in the hydrogel absorbing more molecules and raising the sample's mechanical resistance.

Table 2 shows the US, YM of PAA hydrogel at 300 K and 1 bar after 10 ns in terms of hydrogel atomic ratio. PAA, with a 15 % atomic ratio, had the highest US with 0.0425 MPa, and the highest YM with 0.0014 Mpa.

Conclusion

In this work, we studied the MP of PAA using MD method. The study used the LAMMPS software in conjunction with supplementary modeling and visual applications. The current study included two areas of technical analysis: the examination of equilibrium atomic structures and the evaluation of their mechanical behavior. The results of the equilibration of atomic samples showed that:

- The potential energy in the sample converged to −43 kcal/mol.
- The total energy of the atomic samples reached 12488 kcal/mol.

After equilibrium, the atomic samples MP were investigated.

- The US of the sample was 0.0333 MPa
- The value of calculated YM for PAA was 0.0009 MPa.
- By increasing the atomic ratio of the structure in the range of 5 % to 15 %, the US value increased from 0.0333 MPa to 0.0425 MPa.

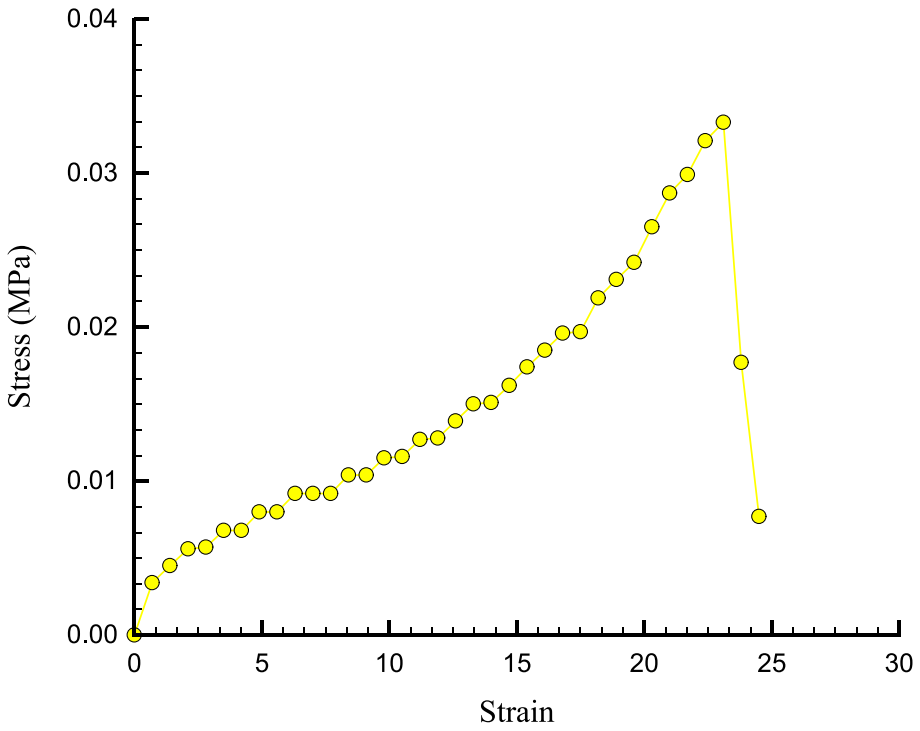

Fig. 4. Stress–strain of the PAA at 300 K and 1 bar.

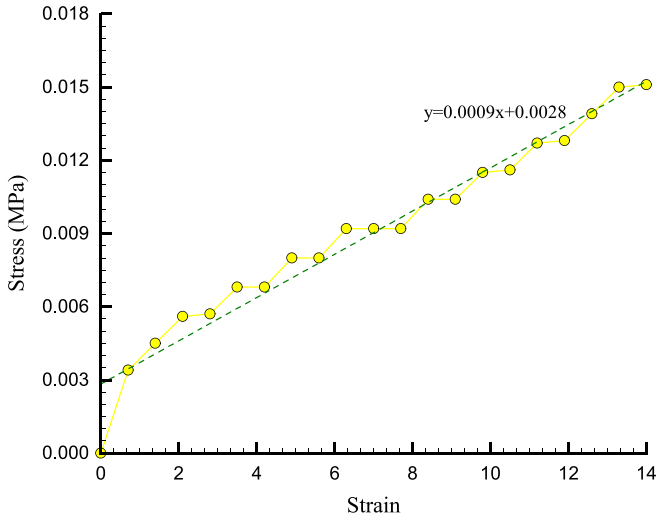

Fig. 5. The YM of the PAA at 300 K and 1 bar.

Table 1
US, YM of PAA at 300 K and 1 bar after 10 ns.

Hydrogel	US (Mpa)	YM (Mpa)
PAA	0.0333	0.0009

- The value of YM reached its maximum from 0.0009 MPa to 0.0014 MPa.

Appendix A. MD method

To characterize the particle's mechanical behavior, the MD simulation conveyed the particle's spatial location, as explained in the following equation [20]:

CRediT authorship contribution statement

Narges Karimzadeh Dehkordi: Investigation, Writing – original draft. **Shahrokh Shojaei:** Investigation, Writing – original draft, Validation, Methodology, Conceptualization. **Azadeh Asefnejad:** Formal analysis, Writing – original draft, Validation, Methodology, Conceptualization. **Kamran Hassani:** Supervision, Writing – review & editing, Validation, Methodology, Conceptualization. **Soheila Zamanlui Benisi:** Validation, Methodology, Conceptualization, Data curation, Formal analysis.

Declaration of competing interest

The authors declare that they have no known competing financial interests or personal relationships that could have appeared to influence the work reported in this paper.

Data availability

No data was used for the research described in the article.

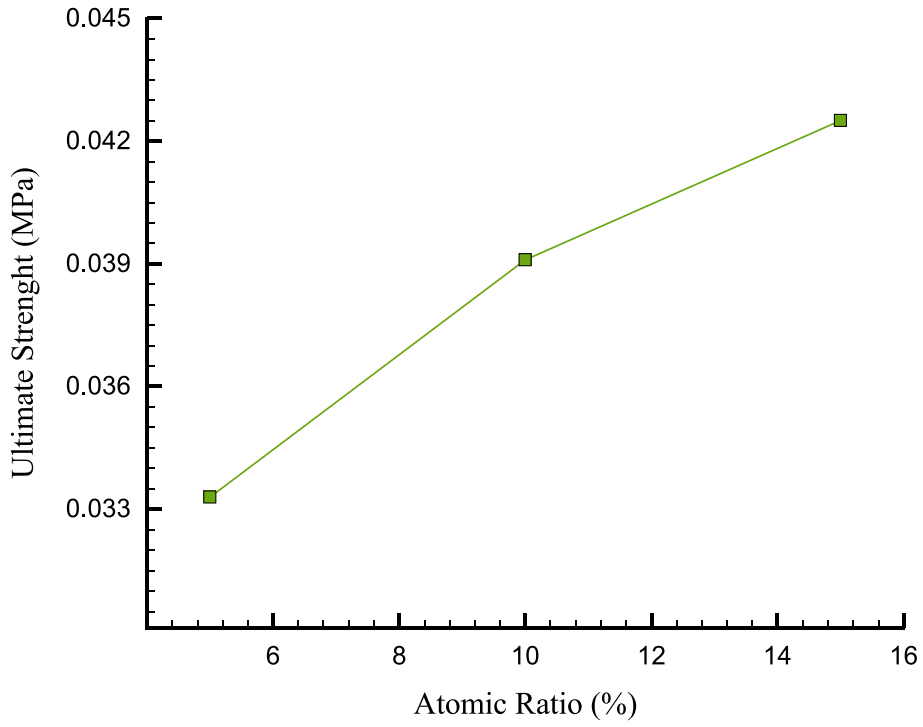

Fig. 6. US of simulated PAA in terms of atomic ratio at 300 K and 1 bar.

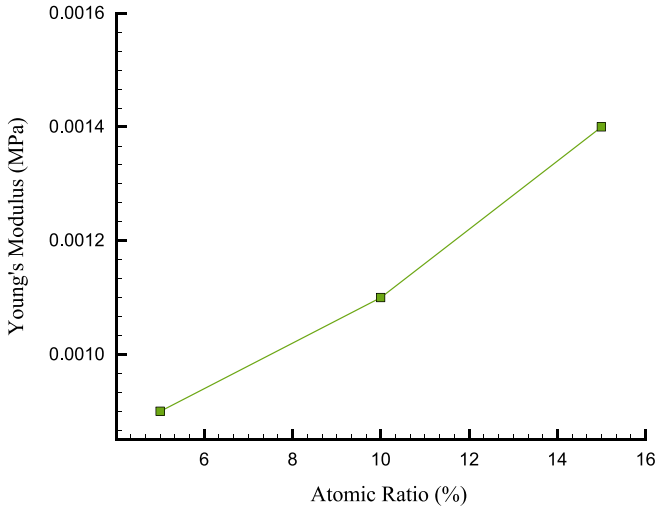

Fig. 7. The YM diagram of the simulated PAA hydrogel sample in terms of atomic ratio at 300 K and 1 bar.

Table 2
US, YM of PAA hydrogel at 300 K and 1 bar after 10 ns in terms of hydrogel atomic ratio.

Atomic ratio (%)	US (Mpa)	YM (Mpa)
5	0.0333	0.0009
10	0.0391	0.001
15	0.0425	0.0014

$$F_i = m_i a_i = m_i \frac{d^2 \boldsymbol{r}_i}{dt^2} \tag{a-1}$$

In above equation, F_i, $\mathbf{r}_i$, m_i, and a_i show the force, the mass of particle i, the spatial position, and particle acceleration, respectively. F_i is obtained by the negative derivative of potential function U concerning the particle position function i as Eq. (a-2) [20]:

$$F_i = -\frac{\partial U}{\partial r_i} \tag{a-2}$$

The selection of a potential atomic function is crucial in MD modeling. Due to the potential energy function of each atom, every other atom in a system may interact with it. Bonded and non-bonded atoms were subjected to this potential energy effect. Bonded atoms have potential, and each atom's potential with other atoms in the same molecule or atoms in nearby molecules is different. Consequently, the bonded and non-bonded interactions imparted to the elements must be combined in order to evaluate the potential energy [20]:

$$E_{total} = E_{bonded} + E_{nonbonded} \tag{a-3}$$

The simulation process was carried out using LAMMPS software. This software considers the molecular structure of a box on a scale, as well as the molecules in the material, the crystal lattice, location and velocity, atom number, potential function coefficients, as well as other molecular properties. Based on the intermolecular forces calculated using potential functions, the atoms move and interact within the simulation box for a predetermined amount of time. As a result of combining Lennard-Jones potentials and Coulomb potentials, a potential function was derived. Eq. (a-4) contains the equation for Lennard-Jones potential function [21,22]:

$$U_{LJ} = 4\varepsilon_{ij}\left[\left(\frac{\sigma_{ij}}{r}\right)^{12} - \left(\frac{\sigma_{ij}}{r}\right)^{6}\right] \tag{a-4}$$

where, ε_{ij} is the depth of potential well, and σ_{ij} is the finite distance in which the potential was zero, The numerical values of ε_{ij} and σ_{ij} for all particles are reported in Table a-1. The cut-off ratio of all particles was considered to be 12 Å. On the other hand, the bond energy, and distance among the atoms at the common surface with each other were computed using the data in Table a-1 and Eqs. (a-5) and (a-6). The values for all interplays among the particles shown in the simulation box were calculated using the Lorentz-Bertolt mixing rule [23].

$$\varepsilon_{ij} = \sqrt{\varepsilon_i \varepsilon_j} \tag{a-5}$$

$$\sigma_{ij} = \frac{\sigma_i + \sigma_j}{2} \tag{a-6}$$

Table a-1. Lennard-Jones potential parameters of present particles [23,24].

	σ_{ij} (Å)	ε_{ij} (kcal/mol)
$N_{acylamino}$-H_{water}	3	3
$O_{acylamino}$-H_{water}	3	2

Electrical PE or electrostatic PE were obtained from the Coulomb equation of constant forces and are represented as follows [25]:

$$U_{ij}(r) = \frac{-1}{4\pi\varepsilon_0}\frac{q_i q_j}{r_{ij}^2} \tag{a-7}$$

where q_i and q_j are electric charges i and j, $r_{ij,}$ the distance among the charges and ε_0 represent the electrical permeability of the open space which are numerically equivalent to 8.85×10^{-12} F·m $^{-1}$.

Using MD simulations, scientists may study the phenomena that were difficult to discover via experimentation, leading to a greater comprehension of the basic principles and processes dictating the behavior of structures. Although MD simulations were useful in expanding our knowledge of material properties, it's critical to recognize their limits. The limitations of using MD simulation in research are as follows:

1. *Computational Resources:* MD simulations need substantial computational resources, such as high-performance computing clusters or supercomputers, to effectively manage the extensive number of atoms and intricate interactions present in the systems. This may impose constraints on the magnitude and duration of simulations that can be executed.
2. *Simplified Models:* Simulations use approximations and simplifications to correctly depict complex processes. Using force fields and potential models in MD simulations was subjected to inherent limitations, and the accuracy of obtained findings was contingent upon the selection of appropriate models and parameterization. For the next simulations, the following assumptions will be used to enhance computational efficiency and streamline complexity:
   - The pressure in all parts of the simulation box was considered constant and uniform.
   - The temperature was considered constant and uniform in all parts of the simulation box.
   - The energy loss among the simulated atomic structures was ignored.
   - The effect of gravitational force in the simulated atomic structures was ignored.
3. *Time Scale Limitations:* Although MD simulations had the capacity to simulate longer time scales compared to experiments, effectively replicating the whole hydration process of concrete, which occurred over a period of weeks to months, remained a tough task. Opting for an excessively short time step resulted in an impractical simulation duration, while selecting a too large time step led to an inaccurate representation of the system (or, in the case of an algorithm like SHAKE, a failure in maintaining the desired constraints). The specific types of structural interactions that we wanted to investigate, such as hydrogen bonding, conformational changes, and binding interactions, each had their own unique time scale. These interactions affected the selection of the appropriate time step [26]. It was not very sensitive to the size of the system (box size). While the time scale for studying conformational changes might range from a few seconds to less than a nanosecond, the size of the molecule was reliant on this process [27]. A time step of 1 fs was determined to be suitable for hydrogels according to the study's results [17].
4. *Uncertainty in Parameters:* Precise parameterization of force fields and potential models was essential for achieving dependable outcomes. A major limitation of the MD method was the lack of assurance about convergence. This issue may be corrected or mediated by doing many separate iterations. In MD simulation, convergence was generally defined as the identification of a set of atomic coordinates that correspond to a local energy

minimum inside the selected force field [28]. The concept of convergence in MD simulation was rooted in the "Ergodic Hypothesis," which stated that the long-term average of a system was equivalent to the average of the ensemble when the ensemble had an unlimited number of members [29]. As mentioned before, the outcome was contingent upon the specific number under consideration. The convergence of energy was included in potential, kinetic, and total energy, as well as temperature, etc. An investigation was conducted on the convergence of total energy and potential energy.

5. *Complexity of Interactions:* To accurately simulate the intricate interactions among various components, such as interfaces and additives, advanced modeling approaches and precise depiction of intermolecular forces were necessary. Creating precise models for complex systems was a continuous challenge in MD simulations [30,31].

References

[1] Sánchez-Cid P, Jiménez-Rosado M, Romero A, Pérez-Puyana V. Novel trends in hydrogel development for biomedical applications: a review. Polymers 2022;14 (15):3023.

[2] Liu Y, Wang J, Chen H, Cheng D. Environmentally friendly hydrogel: a review of classification, preparation and application in agriculture. Sci Total Environ 2022; 846:157303.

[3] Zeng Z, Zhu M, Chen L, Zhang Y, Lu T, Deng Y, et al. Design the molecule structures to achieve functional advantages of hydrogel wound dressings: advances and strategies. Compos B Eng 2022:110313.

[4] Morkhande V, Pentewar R, Gapat S, Sayyad S, Amol BD, Sachin B, et al. A review on hydrogel. Indo Am J Pharm Res 2016;6(3):4678–88.

[5] Ganji F, Vasheghani FE. Hydrogels in controlled drug delivery systems; 2009.

[6] Kalia S. Polymeric hydrogels as smart biomaterials. Springer; 2016.

[7] Nagam SP, Jyothi AN, Poojitha J, Aruna S, Nadendla R. A comprehensive review on hydrogels. Int J Curr Pharm Res 2016;8(1):19–23.

[8] Garcıa D, Escobar J, Bada N, Casquero J, Hernáez E, Katime I. Synthesis and characterization of poly (methacrylic acid) hydrogels for metoclopramide delivery. Eur Polym J 2004;40(8):1637–43.

[9] Jafari A, Hassanajili S, Ghaffari F, Azarpira N. Modulating the physico-mechanical properties of polyacrylamide/gelatin hydrogels for tissue engineering application. Polym Bull 2022:1–22.

[10] Olăreț E, Voicu ȘI, Oprea R, Miculescu F, Butac L, Stancu I-C, et al. Nanostructured polyacrylamide hydrogels with improved mechanical properties and antimicrobial behavior. Polymers 2022;14(12):2320.

[11] Allen MP, Tildesley DJ. Computer simulation of liquids. Oxford University Press; 2017.

[12] Dehkordi RB, Toghraie D, Hashemian M, Aghadavoudi F, Akbari M. Molecular dynamics simulation of ferro-nanofluid flow in a microchannel in the presence of external electric field: effects of Fe3O4 nanoparticles. Int Commun Heat Mass Transfer 2020;116:104653.

[13] An M, Demir B, Wan X, Meng H, Yang N, Walsh TR. Predictions of thermo-mechanical properties of cross-linked polyacrylamide hydrogels using molecular simulations. Advanced Theory and Simulations 2019;2(3):1800153.

[14] Xu P, Shang Z, Yao M, Ke Z, Li X, Liu P. Molecular insights on the mechanical properties of double-network hydrogels reinforced by covalently compositing with silica-nanoparticles. J Mol Liq 2022;368:120611.

[15] Dehkordi NK, Shojaei S, Asefnejad A, Hassani K, Benisi SZ. The effect of three types of cross-linked hydrogels and volume fraction of polyacrylamide on the swelling and thermal behavior using molecular dynamics simulation. J Mater Res Technol 2023;24:4627–38.

[16] Liu F, Wu D, Hong W. Mechanism study on mechanical properties of physical-chemical hybrid hydrogels by coarse-grained molecular dynamics simulations. ACS Appl Polym Mater 2023;5(3):1707–14.

[17] Shahshahani S, Shahgholi M, Karimipour A. The thermal performance and mechanical stability of methacrylic acid porous hydrogels in an aqueous medium at different initial temperatures and hydrogel volume fraction using the molecular dynamics simulation. J Mol Liq 2023;382:122001.

[18] Karoyo AH, Wilson LD. A review on the design and hydration properties of natural polymer-based hydrogels. Materials 2021;14(5):1095.

[19] Caló E, Khutoryanskiy VV. Biomedical applications of hydrogels: a review of patents and commercial products. Eur Polym J 2015;65:252–67.

[20] Rapaport DC. The art of molecular dynamics simulation. Cambridge University Press; 2004.

[21] Oluwajobi A, Chen X. The effect of interatomic potentials on the molecular dynamics simulation of nanometric machining. Int J Autom Comput 2011;8(3): 326.

[22] Von Solms N, O'lenick R, Chiew Y. Leonard-Jones chain mixtures: variational theory and Monte Carlo simulation results. Mol Phys 1999;96(1):15–29.

[23] Berendsen H, Grigera J, Straatsma T. The missing term in effective pair potentials. J Phys Chem 1987;91(24):6269–71.

[24] Rappé AK, Casewit CJ, Colwell K, Goddard III WA, Skiff WM. UFF, a full periodic table force field for molecular mechanics and molecular dynamics simulations. J Am Chem Soc 1992;114(25):10024–35.

[25] Huray PG. Maxwell's equations. John Wiley & Sons; 2011.

[26] Fincham D. Choice of timestep in molecular dynamics simulation. Comput Phys Commun 1986;40(2–3):263–9.

[27] Macgowan D, Heyes DM. Large timesteps in molecular dynamics simulations. Mol Simul 1988;1(5):277–97.

[28] Smith LJ, Daura X, van Gunsteren WF. Assessing equilibration and convergence in biomolecular simulations. Proteins: Struct Funct Bioinf 2002;48(3):487–96.

[29] Henriksson A. On the ergodic theorem and information loss in statistical mechanics; 2019.

[30] Yan S-R, Shirani N, Zarringhalam M, Toghraie D, Nguyen Q, Karimipour A. Prediction of boiling flow characteristics in rough and smooth microchannels using molecular dynamics simulation: Investigation the effects of boundary wall temperatures. Journal of Molecular Liquids 2020;306(112937):112937. https://doi.org/10.1016/j.molliq.2020.112937.

[31] Jolfaei NA, Jolfaei NA, Hekmatifar M, Piranfar A, Toghraie D, Sabetvand R, et al. Investigation of thermal properties of DNA structure with precise atomic arrangement via equilibrium and non-equilibrium molecular dynamics approaches. Computer Methods and Programs in Biomedicine 2020;185(105169): 105169. https://doi.org/10.1016/j.cmpb.2019.105169.